



Published in final edited form as:

ChemMedChem. 2016 November 21; 11(22): 2534–2546. doi:10.1002/cmdc.201600439.

Design and synthesis of fluorescent acyclic nucleoside phosphonates as potent inhibitors of bacterial adenylate cyclases

Petra B ehová^a, Markéta Šmídková^a, Jan Skácel^a, Martin Dra ínský^a, Helena Mertlíková-Kaiserová^a, Monica P. Soto Velasquez^b, Val J. Watts^b, and Zlatko Janeba^a

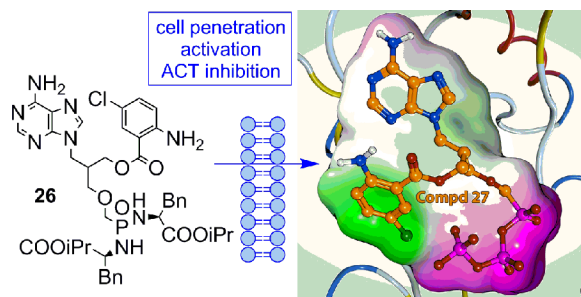
^aThe Institute of Organic Chemistry and Biochemistry of the Czech Academy of Sciences, Flemingovo nám. 2, CZ-166 10 Prague 6, Czech Republic

^bDepartment of Medicinal Chemistry and Molecular Pharmacology, College of Pharmacy, Purdue University, 575 Stadium Mall Drive, West Lafayette, IN – 47907, USA

Abstract

Bordetella pertussis adenylate cyclase toxin (ACT) and *Bacillus anthracis* edema factor (EF) are key virulence factors with adenylate cyclase (AC) activity that substantially contribute to the pathogenesis of whooping cough and anthrax, respectively. There is an urgent need to develop potent and selective inhibitors of bacterial ACs with prospects for development of potential antibacterial therapeutics and to study their molecular interactions with the target enzymes. Novel fluorescent 5-chloroanthraniloyl-substituted acyclic nucleoside phosphonates (Cl-ANT-ANPs) were designed and synthesized in the form of their diphosphates (Cl-ANT-ANPpp) as competitive ACT and EF inhibitors with submicromolar potency (IC₅₀ values 11 – 622 nM). Fluorescence experiments indicated that Cl-ANT-ANPpp analogues bind to the ACT active site and docking studies suggested that the Cl-ANT group interacts with Phe306 and Leu60. Interestingly, the increase of direct fluorescence with Cl-ANT-ANPpp having an ester linker was strictly CaM-dependent, whereas Cl-ANT-ANPpp analogues with an amide linker, upon binding to ACT, increased the fluorescence even in the absence of CaM. Such a dependence of binding on structural modification could be exploited in the future design of potent inhibitors of bacterial ACs. Furthermore, one Cl-ANT-ANP in the form of a bisamidate prodrug was able to inhibit *B. pertussis* ACT activity in macrophage cells with IC₅₀ = 12 μM.

Graphical Abstract



Introduction

Whooping cough, or pertussis, is caused by a strictly human pathogen, *Bordetella pertussis* which is transmitted from infected to susceptible individuals through droplets by coughing or sneezing. Pertussis cases and deaths are reported annually among children and adults despite high vaccination coverage among infants in many countries.^[1] According to WHO estimates in 2008 about 16 million cases of pertussis occurred worldwide, 95% of which were in developing countries and about 195,000 children died from this disease.^[2] The highest incidence and mortality rate is among infants and children less than 12 months old.^[3]

Pertussis is generally treated with antibiotics.^[4] Macrolide antibiotics have been effective and constitute the mainstay of such treatment. Antibiotic treatment is effective in the first catarrhal stage, which is manifested by signs and symptoms resembling various viral infections and a pertussis diagnosis is frequently overlooked. However, antibiotic treatment in the later paroxysmal and convalescence stages is still recommended to clear the nasopharynx of *B. pertussis* and to prevent further spread of the infection. Antimicrobial resistance to *B. pertussis* has been reported sporadically.^[3,5] Immunity to pertussis, acquired from natural infection or through vaccination, is not lifelong. Pertussis infection yields 3 to 30 years of protection and the estimated protection from the pertussis vaccine is 4 to 14 years depending on the vaccine. The whole-cell vaccine generally yields longer protection than the acellular vaccine. The severity of the disease is linked to the time since previous vaccination or illness.^[3,6] Thus, the need for novel treatment strategies to treat pertussis still persists. One of the possible mechanisms to combat *B. pertussis* infections is the inhibition of one or more of the virulence factors of *B. pertussis*.

The calmodulin-dependent adenylate cyclase toxin (ACT) is considered an important virulence factor for *B. pertussis*.^[7] This bifunctional hemolysin/adenylate cyclase protein consists of the N-terminal adenylate cyclase (AC) domain and the C-terminal RTX (Repeats in toxin cytolysin) hemolysin domain.^[8] ACT binds to the surface receptors on phagocytes and translocates its AC domain into the cytosol. The endogenous Ca²⁺-sensor calmodulin (CaM) binds to ACT with high affinity which results in massive production of the cyclic AMP (cAMP) in host cells.^[9] It causes nearly a 1,000-fold increase in the intracellular levels of cAMP and elevation of intracellular [Ca²⁺]_i level.^[10] The increase of cAMP inhibits phagocyte function and facilitates infection of respiratory tract by *B. pertussis* and other possible secondary pathogens.

Acyclic nucleoside phosphonates (ANPs)^[11] are established nucleotide analogues with a broad spectrum of biological activities. The most pronounced is their antiviral effect,^[12] however ANPs exhibit also cytostatic,^[13] antibacterial,^[14] antiparasitic,^[15] and immunomodulatory activities.^[16] Adefovir diphosphate (PMEApp, Figure 1), the active cellular metabolite of adefovir dipivoxil (bis(POM)PMEA) approved for the treatment of chronic hepatitis B virus infection, inhibits *Bordetella pertussis* ACT^[17] and *Bacillus anthracis* edema factor (EF),^[18] both having adenylate cyclase activity. PMEAs and its triphosphate derivatives were also described to inhibit rat brain adenylate cyclase activity.^[19] Furthermore, 2-substituted PMEAs proved to inhibit *B. pertussis* ACT, with

promising selectivity for ACT over mammalian ACs and no cytotoxicity.^[20] It was also shown that cell-permeable bisamidate prodrugs of PMEAs bearing bis(L-phenylalanine isopropyl ester) moiety and its 2-substituted derivatives inhibited ACT effectively in cellular models. Although these bisamidate prodrugs did not inhibit ACT *in vitro* as effectively as bis(POM)PMEA, they were significantly less cytotoxic and showed better plasma stability profiles.^[21]

Gille and Seifert discovered (*N*-methyl)anthraniloyl-substituted nucleoside triphosphates, (M)ANT-NTPs (Figure 1) as potent competitive inhibitors of mammalian and bacterial ACs, including ACT.^[22] Bis-Cl- and bis-Br-ANT-ATP and their ITP analogues were the most potent derivatives known, displaying 50- to 150-fold better selectivity for ACT over mACs.^[22]

Based on the crystal structure of ACT with PMEApp (1ZOT),^[17] we have proposed structures of new acyclic nucleoside phosphonates (ANPs) bearing 5-Cl-ANT substituent at 2' position of the aliphatic side chain attached via variable linkers (Figure 1). Compared to (M)ANT-NTPs, which are suitable for studies of binding interactions with enzymes but are not therapeutically applicable due to their rapid degradation *in vivo*, ANPs are chemically and enzymatically stable phosphate analogues, which can be phosphorylated *in vivo* to their diphosphate forms. Thus, ANPs bearing anthraniloyl moiety may benefit both from their increased biological stability (compared to the natural nucleotides) and from their improved binding affinity to the enzyme (compared to standard ANPs) *via* additional interaction(s) of the aromatic moiety with the lipophilic pocket in the enzyme active site.

In the present study, we describe synthesis of racemic acyclic nucleoside phosphonates bearing 5-chloro-anthraniloyl substituent attached through various linkers (-O-, -NH-, -OCH₂-, -NCH₂-) to the acyclic chain of ANPs. Acyclic nucleoside phosphonate diphosphates (ANPpp), as nucleoside triphosphate analogues, were prepared for their evaluation in the enzyme assays and for fluorescence experiments. On the other hand, for *in vitro* and/or *in vivo* screening of biological properties, the polar phosphonate moiety of ANPs had to be masked by lipophilic prodrugs to facilitate their transport across cell membranes and, thus, improve their potential bioavailability. To this end, bis-amidate derivative bearing bis(L-phenylalanine isopropyl ester) moiety was selected as a prodrug for its advantageous stability and toxicity profile.^[20,21]

Since (M)ANT-nucleosides triphosphates are environmentally sensitive probes displaying increased fluorescence and blue shift of the emission maximum upon exposure to a hydrophobic environment,^[23] such analogues can be studied upon binding to the enzyme active site by measuring direct fluorescence and/or fluorescence resonance energy transfer (FRET). From the crystal structure of ACT with PMEApp,^[17] it can be observed that the catalytic site contains hydrophobic residue Phe306. Binding of the (M)ANT-nucleotide analogues to ACT allows hydrophobic interactions between the (M)ANT group and Phe306, resulting in an increased fluorescence signal. Furthermore, the catalytic domain of ACT bears two tryptophan residues, Trp69 and Trp242, located near the catalytic site, which allow the inhibitor-enzyme complex to be studied using FRET.^[24] Both fluorescence experiments and *in silico* studies of (M)ANT nucleotides showed that they bind to the active

site of the enzyme and that hydrophobic interactions significantly contribute to their binding.^[24] Some of the (M)ANT nucleosides were shown to bind to the ACT even in the absence of CaM.^[24]

Results and discussion

Chemistry

Synthesis of the target compounds started from 2',3'-dihydroxypropyladenine^[25] (**1**, Scheme 1) by protection of the primary 3'-OH group with DMTrCl in pyridine and subsequent reaction with 5-chloroisatoic anhydride in the presence of base.^[26] However, upon deprotection of the DMTr group with acetic acid, the anthraniloyl moiety partially migrates from 2'-position to 3'-position to give an inseparable mixture of compounds **3** and **4** (Scheme 1) in a ratio 5:1 and in overall 79% yield. This isomerization was observed with MANT-nucleotides as well.^[22] To prepare anthraniloyl derivative with more stable amidic bond, 2'-amino derivative **5** was prepared in overall 42% yield (3 steps) by conversion of the 2'-OH group to mesylate, azide, and finally to amino group (Scheme 1).^[27] Treatment of compound **5** with 5-chloroisatoic anhydride under the above conditions and subsequent removal of the DMTr group afforded the desired compound **6** in only 12% yield, together with derivative **7** (75%, data not shown), which was formed by the ring opening of 5-chloroisatoic anhydride via an attack of amino derivative **5** at the carbamic acid carbonyl. Similar result was obtained when using TEA instead of NaH as a base. Finally, when compound **5** was treated with 5-chloroisatoic anhydride without any base, the desired derivative **6** was obtained as a major product (84% yield) with only traces (8%) of derivative **7** (Scheme 1).^[28] Compared to ester compound **3**, the amide analogue **6** was stable and did not undergo any isomerization.

As all attempts to alkylate the 3'-OH group of compounds **3** or **6** with tosyl- or halomethylphosphonate were unsuccessful (data not shown), we decided to introduce the phosphonate moiety first, followed by an attachment of the Cl-ANT group later, as depicted in Scheme 2. The synthesis started by a conversion of previously reported 6-chloro derivative **8**^[29] to adenine analogue **9** using ammonia in ethanol.^[30] 2'-Amino derivative **12** was prepared from compound **9** by the same procedure as compound **5** from **2** (Scheme 1). The subsequent reaction of compounds **9** and **12** with 5-chloroisatoic anhydride gave products **10** and **13**, respectively (Scheme 2). Finally, phosphonates **10** and **13** were converted to the corresponding bis-amidates **11** and **14**, respectively, by transsilylation and subsequent treatment with L-phenylalanine isopropyl ester under standard reaction conditions.^[31] For enzymatic assays triphosphate analogue **15** was prepared from **13** employing the standard morpholidate methodology.^[32] We also attempted to prepare the corresponding triphosphate analogue derived from compound **10**, however the desired product proved to be unstable, probably due to formation of more stable cyclic phosphonate,^[29] affording after work up a complex mixture.

Target derivatives with a prolonged linker at 2'-position containing either -CH₂O- or -CH₂NH- linker were prepared in analogy to the above reported series of compounds, starting from racemic compound **16** (Scheme 3).^[33] Treatment of *N*⁶-benzoyl adenine with

compound **16** and NaH in DMF, followed by the removal of isopropylidene moiety with acetic acid (to give **17**) and protection of one of the free hydroxyl groups using TBSCl^[34] afforded derivative **18** (Scheme 3). Debenzoylation of compound **18** gave intermediate **19**, which was further converted into 3'-amino derivative **21** by standard reaction sequence as described above. Then, the Cl-ANT group was introduced into derivatives **19** and **21**, followed by the removal of the TBS groups, to give compounds **20** and **22**, respectively (Scheme 3).

Finally, TBS-protected derivative **18** was alkylated at the 3'-OH group with bis(2-propyl) p-toluenesulfonyloxymethylphosphonate to give compound **23** (Scheme 4). After the TBS group removal, the hydroxyderivative **24** was converted to Cl-ANT derivatives **25** and **28** (Scheme 4) by above described procedures. For biological screening, phosphonates **25** and **28** were converted to their bis-amidates **26** and **29**, respectively, and to their diphosphate analogues **27** and **30** (Scheme 4), respectively.

Biological evaluation

Inhibition of ACT activity in the cell-free assay

The prepared triphosphate analogues **15**, **27** and **30** were tested, along with PMEApp as a standard, for their inhibitory activity towards several bacterial ACs (Table 1): two commercially available adenylate cyclase toxins (from Sigma and Enzo), expressed recombinantly in *E. coli*, and edema factor (EF) from *Bacillus anthracis*.

Compound **15** showed the same inhibitory activity towards both ACTs tested, but it was weaker inhibitor than compounds **27** and **30** (Table 1). Compounds **27** and **30** inhibited ACT from Sigma with similar IC₅₀ (77 and 91 nM, respectively), but there was a difference in inhibition of ACT from Enzo (IC₅₀ 198 and 47 nM, respectively).

Although both ACTs did not differ significantly in enzymatic and inhibitory AC activities measured in the cell-free assays, only the toxin provided by Enzo was able to elicit a high level of cAMP in these assays. Recombinant ACT produced in *E. coli* has been referred to have the equivalent catalytic AC activity to ACT produced by *B. pertussis*. However, expression of ACT in *E. coli* results in reduced hemolytic activity due to differential posttranslational fatty acylation of the hemolysin domain.^[35] Iwaki et al.^[36] reported that hemolysin domain can stimulate translocation of AC domain across cell membrane. Thus, the potential difference between acylation patterns of these two toxins could explain their dissimilar ability to produce cAMP inside the cells. Furthermore, steric effects of hemolysin domain can affect the access of Cl-ANT-ANPpp to the active site and thus cause discrepancies in the IC₅₀ values for these two toxins.

There is a 25% sequence identity between the core domains of EF and ACT.^[17] Since PMEApp was also shown to inhibit EF effectively,^[18] the effect of analogues **15**, **27** and **30** on the catalytic activity of EF was also evaluated. In this case, compound **15** showed the best inhibitory activity towards EF (IC₅₀ = 69 nM), followed by **27** (IC₅₀ = 613 nM) and **30** (IC₅₀ = 140 nM) (Table 1).

Inhibition of ACT in the cell-based assay

All other prepared Cl-ANT derivatives, either without the phosphonate moiety (compounds **3+4**, **6**, **7**, **20**, and **22**) or with the phosphonate moiety in the form of bisamidate prodrugs (compounds **11**, **14**, **26**, and **29**), were tested for their ability to inhibit ACT activity in J774A.1 macrophage cells (Table 2). The bisamidate prodrugs were prepared as diastereoisomeric mixtures, which were not further separated for their biological evaluation. The putative mechanism of bisamidate cleavage has been reported previously.^[21b] Murine macrophage cells J774A.1 were incubated with various concentrations of the tested compounds and subsequently exposed to *B. pertussis* ACT. The cells were lysed, and the amount of cAMP was determined.

Only compound **26**, where the Cl-ANT moiety is attached at 2'-position *via* –CH₂O– linker, showed inhibitory activity towards ACT with IC₅₀ of 12 μM (Table 2). This activity is two orders of magnitude lower than that of the ACT inhibition by analogous bisamidate prodrug of PMEA or its 2-purine substituted derivatives.^[20] Compound **26** exhibited no cytotoxic effect in J774A.1 cells at a concentration of 10 μM for 5h (Table 2).

Although all triphosphate analogues **15**, **27**, **30** inhibited enzyme activity in the cell-free assay efficiently (Table 1), only prodrug **26** (corresponding to **27**) exhibited moderate inhibitory properties in the J774A.1 cellular model. There are several key preconditions for ANPs in their bisamidate prodrug form to be biologically active towards ACT in the cell-based assay: a) penetration of bisamidate prodrug across cellular membranes; b) efficient cleavage of the prodrug moieties to release free phosphonic acid (ANP); and finally c) subsequent double phosphorylation to ANPpp, the analogue of natural nucleoside triphosphate (in our case the analogue of ATP) which exerts the biological activity. Efficiency of all these steps can largely influence the observed inhibitory activity of Cl-ANT-ANPs inside cell.

Isopropyl ester bis(L-phenylalanine) prodrugs of Cl-ANT-ANPs were prepared, because this prodrug moiety displayed optimal stability profiles in both plasma and macrophage homogenate in our previous studies.^[20] Bisamidate prodrugs have been proven to be hydrolyzed by lysosomal carboxypeptidase cathepsinA (CatA),^[37] which is highly expressed in macrophages.^[38] Definitely, the degree of hydrolysis of compounds **11**, **14**, **26** and **29** by this enzyme may differ, as well as the extent of their phosphorylation by kinases.

Fluorescence experiments with Cl-ANT-ANPpp analogues

FRET Experiments with Cl-ANT-ANPpp analogues

In FRET experiments, compounds **15**, **27** and **30** were added first to the buffer, and their autofluorescence as a result of excitation at 280 nm was detected at 430 nm (Figure 2A, dashed lines). When ACT was added, tryptophan and tyrosine fluorescence occurred at 350 nm (Figure 2A, dotted line). Upon addition of CaM, FRET (decrease in emission at 350 nm and increase in emission at 430 nm) occurred (Figure 2A, solid lines). Similar results were observed when FRET experiments were performed using the tryptophan-specific excitation wavelength of 295 nm (Figure 2B).

By determining FRET with Cl-ANT-ANPpp analogues at increasing concentrations after addition of CaM, saturation curves were obtained (Figure 3). Calculated EC₅₀ values were 214 nM for **15**, 61 nM for **27** and 101 nM for **30**, which is in good agreement with the IC₅₀ values for ACT inhibition obtained in the cell-free assay (Table 1).

Direct fluorescence measurements

Tested compounds were excited at 350 nm and emission was scanned from 380 to 550 nm. Addition of ACT to the well containing **27** did not result in increase of its intrinsic fluorescence (Figure 4). Upon the addition of CaM, fluorescence immediately increased by 30% and the emission maximum of **27** showed a shift to shorter wavelengths (Figure 4). There was no change in fluorescence profile during the time (Figure S1). After the addition of ACT to the wells containing **15** and **30**, their fluorescence immediately increased two times and did not change with time (Figure 4, Figure S1). Subsequent addition of CaM led to progressive increase in fluorescence of **15** and **30** by 16 times and 6 times, respectively, within 2 min (Figure 4, Figure S1). These results show that the Cl-ANT moiety apparently interacts with the hydrophobic moiety of Phe306 in the active site of ACT. CaM is essential for the binding of compound **27** to the ACT active site since **27** does not increase fluorescence in the absence of CaM. On the other hand, derivatives **15** and **30** increased fluorescence in the absence of CaM, which shows that these derivatives can bind to the active site even without CaM. However, after addition of CaM, fluorescence dramatically increased suggesting even more effective binding to the enzyme in the presence of CaM.

Inhibition of FRET by PMEApp

PMEApp inhibited FRET in a concentration-dependent manner (Figure 5). Half-maximal displacement of 100 nM **27** and **30** occurred at a PMEApp concentration of 67.05 ± 8.2 nM and 33.26 ± 5.9 nM, respectively. Kinetics of ACT FRET inhibition by PMEApp occurred within the mixing time in the case of **27**. Displacement of **30** by PMEApp was slower than that observed for **27**.

In conclusion, all compounds **15**, **27** and **30** bind to the active site of ACT, as demonstrated by their displacement with PMEApp. Compounds **15** and **30** can bind to ACT in the absence of CaM, although CaM clearly stimulates their binding by an order of magnitude. Compounds **15** and **30** showed similar spectral changes that have been observed for 2,4,6-trinitrophenyl (TNP) nucleotides.^[24] Compound **27** does not bind to ACT in the absence of CaM and it gives similar fluorescence response, and thus probably adopts similar position in the ACT binding site, as MANT nucleotide analogues.^[24]

Molecular modeling of the binding mode of Cl-ANT-ANPpp to ACT

For further investigation of direct molecular space of ligands, docking studies were performed with Molecular Operating Environment (MOE).^[39] The data obtained demonstrate (Figure 6) that the 5-chloroanthraniloyl (Cl-ANT) moiety interacts with Phe306 by C-H- π or possibly π - π interaction (in a distance 3.0Å to 3.1Å). Leu60 can also contribute to the binding of Cl-ANT moiety with C-H- π interaction (2.95–3.0Å). Only (*S*-

stereoisomers of compounds **27** and **30** could be placed into the binding pocket which indicates that only the (*S*)-stereoisomers are binding to the ACT active site and, thus, exert biological effects observed. Unfortunately, attempts to separate the individual stereoisomers of **27**, using capillary electrophoresis with cyclodextrins as chiral selectors,^[40] did not afford enough material for the evaluation of their discrete ACT inhibitory properties.

Another key interaction was observed between Asn304 residue and ester or amide linker of the CI-ANT moiety (average distance of 2.6Å) in compounds **27** (Figure 6) and **30**. The hydrogen bond between amide group of Asn304 and carbonyl of the ester linker apparently promotes strong binding of derivative **27** (Figure 6). Better inhibitory properties of amidic derivatives **15** and **30** in comparison with ester analogue **27** (Table 1), as well as slower displacement of **30** with PMEApp from the active site, can be speculated to be due to the presence of two possible intermolecular amide-amide (C=O...H-N) hydrogen bonds between compounds **15** or **30** and ACT.

Inhibition of mACs

Finally, the ability of the prepared compounds (**3+4**, **6**, **7**, **11**, **14**, **20**, **22**, **26** and **29**) to inhibit host mammalian adenylate cyclases (mACs) was examined (Table 3). The assays were carried out using HEK293 cells stably expressing mAC1, mAC2, or mAC5, and each compound was tested in two independent experiments at 30 µM. These mACs are representatives of the three major families of mACs. Specific activation of the mAC overexpressed in the cells was accomplished by previously reported methodology,^[41] where a calcium ionophore A23187 was employed to stimulate AC1, a PKC activator, phorbol 12-myristate 13-acetate (PMA) to stimulate AC2, and forskolin to stimulate AC5. None of the compounds significantly inhibited any mAC but several compounds (**11**, **14** and **29**) slightly potentiated the selectively-stimulated cAMP response at AC1 and AC2 (Table 3).

Conclusions

A novel series of potent inhibitors of bacterial adenylate cyclases (ACs), namely adenylate cyclase toxin (ACT) from *B. pertussis* and edema factor (EF) from *B. anthracis*, was designed. Three acyclic nucleoside phosphonate diphosphates with the CI-ANT substituent attached to the acyclic side chain (CI-ANT-ANPpp analogues), compounds **15**, **27** and **30**, were successfully prepared, while the corresponding ANPpp derived from compound **10** could not be isolated due to its instability. All three nucleoside triphosphate analogues **15**, **27** and **30** exhibited submicromolar inhibitory activity towards both ACT and EF with their potency comparable to that of (bis)-CI-ANT-NTPs reported by the group of Seifert.^[22] However, adefovir diphosphate (PMEApp) and its 2-substituted analogues still exhibit better inhibitory activities in the low nanomolar range.^[20] The attachment of fluorescent CI-ANT group to potential ACs inhibitors enables an examination of their binding using fluorescence methodology.^[24] The fluorescence experiments with compounds **15**, **27** and **30** showed similar binding to ACT as parent (M)ANT-nucleotides, which indicates their binding to the catalytic site of ACT. Furthermore, molecular docking experiments showed direct interactions of CI-ANT-group with Phe306 and Leu60 in the active site, while the carbonyl

group (C=O) present in the aliphatic linker of the ANPpp inhibitors is able to form an extra hydrogen bond with Asn304.

The ACT catalytic site is formed by a cavity with a substantial freedom to accommodate structurally diverse ligands, for example various purine, as well as pyrimidine nucleotide analogues.^[24] On the other hand, even small structural variation can lead to a surprisingly huge difference in the binding mode of the ACT inhibitors. We have shown that compound **27** requires the presence of CaM to bind to ACT, while the other two potent ACT inhibitors, compounds **15** and **30**, bind to ACT even in the absence of CaM, although CaM clearly stimulates their binding by an order of magnitude. This is an important observation. The results indicate slightly different orientations of the two types of studied CI-ANT-ANPpp analogues (with ester or amide bond in the aliphatic chain) in the ACT catalytic site. Both types of compounds may provide valuable conformational probes to better understand the mechanism of ACT activation and, at the same time, can potentially facilitate the design of future potent and selective ACs inhibitors.

Finally, the corresponding CI-ANT-ANPs **11**, **14**, **26** and **29**, as isopropyl ester bis(L-phenylalanine) prodrugs,^[20,21] were efficiently synthesized for their evaluation in cell-based assays. ACT inhibitory properties of these CI-ANT-ANPs, as well as their acyclic nucleoside intermediates **3+4**, **6**, **7**, **20** and **22**, were studied *in vitro* in J774A.1 macrophages. From the compounds tested, only prodrug **26**, corresponding to the potent triphosphate analogue **27**, exhibited reasonable inhibitory activity towards ACT with an IC₅₀ value of 12 μM and no observed cytotoxic effects in J774A.1 cells. The lack of potent inhibitory properties of the other prepared bisamidate prodrugs of ANPs, together with no observed inhibition of mammalian ACs (mAC1, mAC2 and mAC5) in cell-based assays, may suggest that the released ANPs are not sufficiently phosphorylated in the cells to the active species, i.e. ANPpp derivatives. This issue is going to be addressed in our future research.

In summary, CI-ANT-ANPpp derivatives, acyclic analogues of fluorescent natural nucleoside triphosphates, represent a great tool to study molecular interactions of *B. pertussis* ACT with its substrates and/or potential inhibitors. The data obtained indicate that specific inhibitors can be designed that are able to interact with bacterial cyclases either in the presence or in the absence of CaM. Potent and selective inhibitors of bacterial adenylate cyclases with improved bioavailability may eventually become valuable agents for prophylaxis or reduction of toxemia in highly contagious diseases like pertussis and anthrax.

Experimental Section

Starting compounds and other chemicals were purchase from commercial suppliers or prepared according to the published procedures. Solvents were dried by standard procedures. Solvents were evaporated at 40 °C/2 kPa. Analytical TLC was performed on plates of Kieselgel 60 F₂₅₄ (Merck). NMR spectra were recorded on Bruker Avance 500 (¹H at 500 MHz, ¹³C at 125.8 MHz) and Bruker Avance 400 (¹H at 400 MHz, ¹³C at 100.6 MHz) spectrometers with TMS or dioxane (3.75 ppm for ¹H, 67.19 ppm for ¹³C NMR) as internal standard or referenced to the residual solvent signal. Mass spectra were measured on UPLC-MS (Waters SQD-2). HR MS were taken on a LTQ Orbitrap XL spectrometer. The

microwave-assisted reactions were carried out in CEM Discover (Explorer) microwave apparatus. Preparative HPLC purification of triphosphate analogues was performed on a column packed with POROS® HQ 50 mm (50mL) with use of a gradient of TEAB in water (0.05–0.5 M). The purity of the tested compounds was determined by HPLC (H₂O-CH₃CN, linear gradient) and was higher than 95%.

General procedures

General procedure 1 (GP1)—Reaction of a hydroxy derivative with 5-chloroisatoic anhydride: A hydroxy derivative (1 mmol) in dry DMF (8 mL) was treated with NaH (44 mg, 1.1 mmol) under Ar at RT and the resulting mixture was stirred at room temperature for 30 min. 5-Chloroisatoic anhydride (0.4 g, 2 mmol) was added and the mixture was stirred at 80 °C for 3 h. The reacting mixture was cooled to room temperature and poured to EtOAc (50 mL) and extracted twice with saturated NaHCO₃ (50 mL) and brine (50 mL) and dried over MgSO₄.

General procedure 2 (GP2)—Conversion of hydroxy group to amino group: The hydroxy derivative (1 mmol) was co-evaporated with dry pyridine (1 × 10 mL), dissolved in dry pyridine (10 mL) and treated with MsCl (0.15 mL, 2 mmol) at 0 °C and the reaction mixture was stirred at room temperature for 2 h. MeOH (5 mL) was added at 0 °C and the volatiles were evaporated. The crude product was dissolved in EtOAc (20 mL) and washed with NaHCO₃ (20 mL), brine (20 mL) and dried over MgSO₄. The obtained crude mesylate was without further purification dissolved in DMF/HMPA mixture (1:1, 6 mL) and treated with NaN₃ (325 mg, 5 mmol) at 100 °C overnight, cooled and poured into EtOAc (50 mL), washed with brine (5 × 30 mL) and dried over MgSO₄. The azido derivative was purified by flash chromatography (CHCl₃/MeOH 0–5%). The azide (3.9 mmol) in MeOH (45 mL) was treated with H₂ over Pd/C (10 wt. % loading, 350 mg) under atmospheric pressure for 24 h. The reaction mixture was filtered, evaporated and purified by flash chromatography (CHCl₃/MeOH 0–5%).

General procedure 3 (GP3)—Reaction of amino derivative with 5-chloroisatoic anhydride: The amino derivative (0.3 mmol) in DMF/THF mixture (1:5, 3 mL) was treated with DMAP (3.7 mg, 0.03 mmol) and 5-chloroisatoic anhydride (0.12 g, 0.6 mmol) at room temperature overnight and solvents were evaporated.

General procedure 4 (GP4)—Preparation of the bisamidate prodrugs: Phosphonate diester (1 mmol) was dissolved in dry pyridine (10 mL), and TMSBr (1 mL) was added. The reaction mixture was stirred at room temperature overnight. After evaporation of the volatiles, the flask was purged with Ar (without any contact with air) and amino acid ester hydrochloride (4 mmol, dried in vacuo at 30 °C and 0.1 mbar for 1 day), dry trimethylamine (2 mL) and dry pyridine (8 mL) were added, and the mixture was heated at 70 °C to obtain a homogenous solution. Then, a solution of 2,2'-dipyridyldisulfide (6 mmol) and triphenylphosphine (6 mmol) in dry pyridine (10 mL) was added under Ar. The resulting mixture was heated at 70 °C for 72 h. After cooling to room temperature, the solvent was removed and the residue was purified by flash chromatography (gradient of MeOH (2–30%) in a mixture of hexane/EtOAc, 60:40) to remove impurities, followed by reversed-phase

chromatography on C₁₈ silica gel (aqueous MeOH 1–100%). The products were freeze dried from 1,4-dioxane.

General procedure 5 (GP5)—Synthesis of phosphonate diphosphates: Diisopropyl ester of phosphonic acid (0.1 mmol) in pyridine (2 mL) was treated with TMSBr (0.1 mL) at room temperature overnight. The volatiles were removed under reduced pressure, the residue was co-evaporated with water and suspended in water and the free phosphonic acid was filtered off, dissolved in *t*BuOH and H₂O (1:1, 2 mL) and morpholine (35 μ L) was added. Solution of DCC (82 mg) in *t*BuOH (2 mL) was added dropwise at 80 °C and the resulting mixture was heated at 80 °C until complete conversion of the reaction. The mixture was poured into H₂O/Et₂O mixture and the aqueous phase was washed with Et₂O (3 \times 30 mL), finally Et₂O was washed with water. Collected aqueous phase was evaporated and the residue was co-evaporated with EtOH and dry toluene. The dried residue was treated with tri-*n*-butylammonium pyrophosphate (0.5 M solution in DMSO) at room temperature for 48 h. The reaction mixture was diluted with Et₂O (10 mL), Et₂O layer was poured off and the precipitate was dissolved in 0.05 M TEAB (4 mL) and applied onto a column of POROS® HQ, and eluted with a linear gradient of TEAB (0.05–0.5 M). The fractions containing product were concentrated at 27 °C and the residue was applied onto DOWEX 50 \times 8 (Na⁺ form), eluted with water and freeze dried.

9-[3-O-(4,4'-dimethoxytrityl)-2-hydroxypropyl]adenine (2)—9-(2,3-dihydroxypropyl)adenine (4.18 g, 20 mmol) in dry pyridine (200 mL) was treated with DMAP (35 mg, 0.29 mmol), TEA (2.8 mL, 20 mmol) and DMTrCl (7.53 g, 22 mmol) at room temperature overnight. MeOH (10 mL) was added and the solvent was evaporated, the residue in EtOAc (100 mL) was washed with sat. NaHCO₃ and brine and dried over MgSO₄. The crude product was purified by flash chromatography (CHCl₃ with 0.5% TEA/MeOH 0–5%) to give an off-white foam (6.1 g, 88%).

9-[2-O-(5-Chloroanthraniloyl)-3-hydroxypropyl]adenine (3) and 9-[3-O-(5-chloroanthraniloyl)-2-hydroxypropyl]adenine (4)—Prepared from **2** (708 mg, 1.38 mmol) according to GP1. The crude product was treated with AcOH (80%, 20 mL) at room temperature for 2 h. Acetic acid was evaporated and the resulting crude product was purified by flash chromatography (CHCl₃/MeOH 0–5%) and freeze dried from 1,4-dioxane to give inseparable mixture of compounds **3** and **4** (5:1, 396 mg, 79% overall yield).

9-[2-Amino-3-O-(4,4'-dimethoxytrityl)propyl]adenine (5)—Prepared from **2** by GP2. White foam, overall yield (two steps) 50%. Also, intermediate 9-[2'-azido-3'-O-(4,4'-dimethoxytrityl)propyl]adenine was isolated as a white foam, yield 85%.

9-[2-*N*-(5-Chloroanthraniloyl)-3-hydroxypropyl]adenine (6) and 2-(3-(1-(6-amino-9H-purin-9-yl)-3-hydroxypropan-2-yl)ureido)-5-chlorobenzoic acid (7)—Prepared according to GP3. The crude product was treated with 80% AcOH (10 mL) at room temperature for 3 h. Acetic acid was evaporated and the residue was purified by flash chromatography (CHCl₃/MeOH 0–5%) and freeze dried to give **6** (167 mg, 84%) as a white foam. As a second product compound **7** (10 mg, 8%) was isolated as a white foam.

9-{3-[(Diethoxyphosphoryl)methoxy]-2-hydroxypropyl}adenine (9)—Compound **8** (800 mg, 2.1 mmol) was treated with ammonia in EtOH (15 mL) and heated under microwave irradiation (50 W) at 100 °C for 1 h. The solvent was evaporated and the residue was purified by flash chromatography (CHCl₃/MeOH 0–5%) to give **9** as a colorless oil (550 mg, 72%).

9-{3-[(Diethoxyphosphoryl)methoxy]-2-O-(5-chloroanthraniloyl)propyl}adenine (10)—Prepared from **9** (360 mg, 1 mmol) by GP1 at room temperature, purified by flash chromatography (CHCl₃/MeOH 0–5%) to give yellowish oil (462 mg, 90%).

Bis(L-phenylalanine isopropyl ester) prodrug of ((3-(6-amino-9H-purin-9yl)-2-O-(5-chloroanthraniloyl)propoxy)methyl)phosphonic acid (11)—Prepared from **10** (110 mg, 0.2 mmol) by GP4, white foam (95 mg, 56%).

9-{2-Amino-3-[(diethoxyphosphoryl)methoxy]propyl}adenine (12)—The hydroxy derivative **9** (550 mg, 1.5 mmol) in dry pyridine (10 mL) was treated with MsCl (0.22 mL, 3 mmol) at 0 °C and allowed to stir at room temperature for 2 h. MeOH (5 mL) was added at 0 °C and the volatiles were evaporated. The crude product was dissolved in EtOAc (20 mL) and washed with NaHCO₃ (20 mL), brine (20 mL) and dried over MgSO₄. The mesylate was without further purification dissolved in DMF/HMPA mixture (1:1, 5 mL) and treated with NaN₃ (487 mg, 7.5 mmol) and stirred at room temperature for 3 days, further NaN₃ (487 mg, 7.5 mmol) was added and the mixture was stirred for further 3 days and the resulting mixture was poured into EtOAc (50 mL) and washed with brine (5 × 30 mL) and dried over MgSO₄ and purified by flash chromatography (CHCl₃/MeOH 0–5%) to give 9-{2-azido-3-[(diethoxyphosphoryl)methoxy]propyl}adenine (398 mg, 59%). The azide (190 mg, 0.49 mmol) in MeOH (10 mL) was treated with Pd/C (10 wt. % loading, 15 mg) and H₂ under atmospheric pressure for 24 h. The reaction mixture was filtered, evaporated and purified by flash chromatography (CHCl₃/MeOH 0–30%) to give colorless oil (120 mg, 66%).

9-{3-[(Diethoxyphosphoryl)methoxy]-2-N-(5-chloroanthraniloyl)propyl}adenine (13)—Prepared from **12** (115 mg, 0.32 mmol) by GP3 to give **13** as a colorless oil (130 mg, 79%).

Bis(L-phenylalanine isopropyl ester) prodrug of ((3-(6-amino-9H-purin-9yl)-2-N-(5-chloroanthraniloyl)propoxy)methyl)phosphonic acid (14)—Prepared from **13** (65 mg, 0.126 mmol) by GP4, white foam (58 mg, 54%).

((3-(6-Amino-9H-purin-9yl)-2-N-(5-chloroanthraniloyl)propoxy)methyl)phosphonic acid diphosphate, sodium salt (15)—Prepared from **13** (51.2 mg, 0.1 mmol) by GP5, white foam (12 mg, 17%).

9-(3-Hydroxy-2-(hydroxymethyl)propyl)-N⁶-benzoyladenine (17)—N⁶-benzoyladenine (1.84 g, 7.7 mmol) in dry DMF (25 mL) was treated with NaH (0.372 g, 9.3 mmol, 60% susp. In mineral oil) at 0 °C for 30 min. and compound **16** (2.6 g, 11.6 mmol) in dry DMF (5 mL) was added and the reaction mixture was heated at 60 °C for 24 h. The

resulting mixture was cooled and diluted with EtOAc (200 mL) and washed with brine (3 × 10 mL) and dried over MgSO₄. The crude product was treated with 80% AcOH (25 mL) at 60 °C for 30 min. The mixture was cooled and acetic acid was evaporated and co-evaporated with water and EtOH. Flash chromatography gave **17** (1.3 g, 53%) as a white solid.

9-(3-O-(*t*-Butyldimethylsilyl)-2-(hydroxymethyl)propyl)-N⁶-benzoyladenine (18)

—Dihydroxy derivative **17** (1.48 g, 4.5 mmol) in dry DMF (25 mL) was treated with imidazole (0.46 g, 6.75 mmol) and TBSCl (0.75 g, 4.95 mmol) was added in portions and the resulting mixture was stirred at room temperature for 24 h. The solvent was evaporated and the crude product was purified by flash chromatography (CHCl₃/MeOH 0–10%) to give **18** (1 g, 50%) as a white solid.

9-(3-O-(*t*-Butyldimethylsilyl)-2-(hydroxymethyl)propyl)adenine (19)

—Compound **18** (830 mg, 1.9 mmol) in MeOH (15 mL) was treated with MeONa (2 mL, 1M solution in MeOH) at room temperature overnight. The reaction mixture was neutralized with AcOH and evaporated. The crude product was purified by flash chromatography (CHCl₃/MeOH 0–10%) to give **19** (510 mg, 81%) as a white solid.

9-(3-O-(5-Chloroanthraniloyl)-2-(hydroxymethyl)propyl)adenine (20)

—Prepared from **19** (170 mg, 0.5 mmol) by GP1. The crude product was treated with AcOH (80%, 10 mL) at 50 °C for 8 h. Acetic acid was evaporated, the residue was co-evaporated with water and EtOH and purified by flash chromatography (CHCl₃/MeOH 0–10%) and freeze dried from 1,4-dioxane to give **20** (93 mg, 49%) as a white foam.

9-(2-(Aminomethyl)-3-O-(*t*-butyldimethylsilyl)propyl)adenine (21)

—Prepared from **20** (120 mg, 0.36 mmol) by the same procedure as compound **12**. Intermediate 9-(2-(azidomethyl)-3-O-(*t*-butyldimethylsilyl)propyl)adenine was obtained as a white solid (110 mg, 85%). The amino derivative (**21**) was obtained as a white solid (35 mg, 34%).

9-(3-N-(5-Chloroanthraniloyl)-2-(hydroxymethyl)propyl)adenine (22)

—Prepared from **21** (35 mg, 0.1 mmol) by GP3. The crude product was treated with AcOH (80%, 5 mL) at 60 °C for 3 h. The solvent was evaporated, co-distilled with water and EtOH and the residue was purified by flash chromatography (CHCl₃/MeOH 0–10%) and freeze dried from 1,4-dioxane to give **22** (27 mg, 53%) as a white foam.

9-(3-O-(*t*-Butyldimethylsilyl)-2-(diisopropoxyphosphorylmethoxymethyl)propyl)-N⁶-benzoyladenine (23)

—Compound **18** (0.5 g, 1.13 mmol) in DMF (10 mL) was treated with (*t*BuO)₂Mg (0.29 g, 1.7 mmol) and *p*TsOCH₂P(O)(OiPr)₂ (0.54 g, 1.7 mmol), and the reaction mixture was heated at 60 °C for 3 days. The mixture was cooled to room temperature, diluted with EtOAc (100 mL), washed with brine (3 × 10 mL) and dried over MgSO₄. The product was purified by flash chromatography (CHCl₃/MeOH 0–5%), colorless oil (380 mg, 44%).

9-[2-(Hydroxymethyl)-3-(diisopropoxyphosphorylmethoxy)propyl]adenine (24)

—Compound **23** (1.14 g, 1.8 mmol) in dry THF (50 mL) was treated with TBAF (1M solution in THF, 4 mL) at room temperature overnight, evaporated, dissolved in EtOAc and

washed with brine and dried over MgSO_4 to give a colorless oil: MS-ESI m/z (%): 506.16 (100) $[M+H]^+$. The crude product was dissolved in MeOH (15 mL) and treated with MeONa (1M solution in MeOH, 3 mL) at room temperature for 6 h. The reaction mixture was neutralized with AcOH, evaporated and purified by flash chromatography ($\text{CHCl}_3/\text{MeOH}$ 0–5%). Compound **24** was obtained as a colorless oil (598 mg, 81%).

9-[2-(5-Chloroanthraniloyloxymethyl)-3-(diisopropoxyphosphorylmethoxy)propyl]adenine (25)—Prepared from derivative **24** (400 mg, 1 mmol) by GP1, colorless oil (410 mg, 74%).

Bis(L-phenylalanine isopropyl ester) prodrug of ((3-(6-amino-9H-purin-9yl)-2-(5-chloroanthraniloyloxymethyl)propoxy)methyl)phosphonic acid (26)—Prepared from **25** (110 mg, 0.2 mmol) by GP4 to give **26** (95 mg, 56%) as a white foam.

((3-(6-Amino-9H-purin-9yl)-2-(5-chloroanthraniloyloxymethyl)propoxy)methyl)phosphonic acid diphosphate, sodium salt (27)—Prepared from **25** (55 mg, 0.1 mmol) by GP5, white foam, yield 29 mg (41%).

9-[2-(5-Chloroanthraniloylaminoethyl)-3-(diisopropoxyphosphorylmethoxy)propyl]adenine (28)—The hydroxy derivative **24** (570 mg, 1.4 mmol) was converted to 9-[2-(azidomethyl)-3-(diisopropoxyphosphorylmethoxy)propyl]adenine (280 mg, 46%) and further to 9-[2-(aminomethyl)-3-(diisopropoxyphosphorylmethoxy)propyl]adenine (130 mg, 51%) by the same procedure as was described for compound **12**. The amino derivative (120 mg, 0.3 mmol) was finally converted by GP3 to **28** (140 mg, 84%).

Bis(L-phenylalanine isopropyl ester) prodrug of ((3-(6-amino-9H-purin-9yl)-2-(5-chloroanthraniloylaminoethyl)propoxy)methyl)phosphonic acid (29)—Prepared from **28** (70 mg, 0.126 mmol) by GP4 to give **29** (70 mg, 65%) as a white foam.

((3-(6-Amino-9H-purin-9yl)-2-(5-chloroanthraniloylaminoethyl)propoxy)methyl)phosphonic acid diphosphate, sodium salt (30)—Prepared from **28** (55 mg, 0.1 mmol) by GP5, white foam, yield 12 mg (17%).

Molecular Docking—Crystal structure of *Bordetella pertussis* adenylyl cyclase toxin with CAM and PMEApp (PDB code 1ZOT, resolution 2.2Å)^[17] was prepared with MOE Ligx with default setup and structure was minimized to RMS gradient of 0.001. Structures of all final compounds above were properly protonated and deprotonated and minimized to RMS gradient of 0.001. For docking studies rigid dock protocol was chosen with structure waters included and ligands rotate bonds was enabled. Default placement and refinement method was used with 50 retained structures after the first refinement and 20 retained structures after the second refinement. As positions of nucleobases in enzymes are typically highly conserved, pharmacophore restraints were applied for nucleobase (features volume in brackets): both aromatic rings (1.3), hydrogen donor to backbone oxygen of Thr300 (1.5),

hydrogen acceptor from water1030 to nitrogen N1 of purine (1.3). For all calculations Amber12:EHT mixed forcefield was used with Generalized Born solvent model.

Biological assays

Effect on the viability of J774A.1 cells—J774A.1 cells were plated onto white 96-well assay plates at 5×10^4 cells per well and allowed to attach overnight. Cells were then washed with HBSS and treated with 10 μM compounds for 5 h. Cell viability was then assessed with a Cell Titer-Glo Luminescent Cell Viability assay (Promega, Madison, WI, USA) according to the manufacturer's instructions. Measurement of luminescence signal was performed by use of a GENios microplate reader (Tecan Systems). Data were expressed as percent of control, represented by untreated cells.

Inhibition of ACT – cell-based assay—J774A.1 cells were seeded in a 96-well plate at 5×10^4 cells per well and left to attach overnight. Prior to the experiment, cells were washed with HBSS (135 mM NaCl, 5.9 mM KCl, 1.5 mM CaCl_2 , 1.2 mM MgCl_2 , 25 mM glucose, 10 mM HEPES [pH 7.4]) and pre-incubated with compounds at concentrations of 0.001–30 μM for 5 h. After that, cells were exposed to ACT (2 nM) from *B.pertussis* (Enzo Life Sciences, Palo Alto, CA; SA=115 $\mu\text{mol}/\text{min}/\text{mg}$) for 30 min. Finally, the cAMP content was determined by using the CatchPoint cAMP immunoassay kit (Molecular Devices, Wokingham, UK). After the addition of lysis buffer (50 μL per well) provided by the manufacturer, the cellular content was extracted by shaking the plate at 250 rpm for 10 min. The plate was then centrifuged to remove cell debris, the supernatant was replaced to the assay plate, and immunoassays were carried out according to the manufacturer's instructions. Fluorescence signal was acquired using an Infinite M1000 plate reader (Tecan Systems Inc., San Jose, CA, USA).

Inhibition of ACT – cell-free assay—In a cell-free assay, AC enzymatic activity was measured by conversion of [^3H] ATP to [^3H]cAMP. The reaction was carried out at 30°C for 30 min, with a final reaction volume of 50 μL . Each assay mixture contained 3 μM BSA, 20 mM HEPES (pH 7.4), 10 mM MnCl_2 , 1 mM EDTA, 1 μM CaCl_2 , 0.1 mM cold ATP, 20 μCi [2,8- ^3H]ATP (ARC, St. Louis, MO, USA; specific activity 20 Ci/mmol), 1.2 μM calmodulin and tested compound at concentration of 0 – 100 μM . Inhibition of AC activity was determined in the presence of 3 different enzymes ACT (Sigma, specific activity 65 $\mu\text{mol}/\text{min}/\text{mg}$), ACT (Enzo, specific activity 115 $\mu\text{mol}/\text{min}/\text{mg}$) and EF (LBL, specific activity 830 $\mu\text{mol}/\text{min}/\text{mg}$) with the final enzyme concentration of 1.1 nM, 0.67 nM and 0.12 nM, respectively. The incubation was carried out for 30 min at 30°C, in a final reaction volume of 50 μL . A 2 μL aliquot of the assay mixture was spotted on a polyethylenimine chromatographic sheet, and developed in 4M LiCl:1 M acetic acid (1:4). After developing, the spots containing ATP and cAMP were quantified using Radio-TLC scanner RITA (RAYTEST, Germany) with evaluation software GINA STAR TLC. Data were calculated from the percentage conversion of [^3H]ATP to [^3H]cAMP. K_i values were calculated using the Graphpad Prism 5 software (San Diego, CA, USA). All assays were performed in duplicate with three independent repetitions. In statistical analysis, Student's *t* test (two-sided) was used. Results are given as means \pm SD.

Fluorescence spectroscopy—The measurements were carried out in black 96-well plates (Nunc) at 25°C using the Cytation 3 microplate reader (BioTek, VT, USA). The final assay volume was 75 μ l. Reaction mixtures contained a buffer consisting of 100 μ M CaCl₂, 100 mM KCl, 5 mM MnCl₂, and 75 mM HEPES, pH 7.4. Further, 2-(CI-ANT)-ANPpp compounds, ACT and CaM were added successively. In FRET experiments, 2-(CI-ANT)-ANPpps were used at final concentrations from 10 nM to 500 nM, and ACT and CaM were 300 nM each. Steady-state emission spectra were recorded at low speed with and λ_{ex} = 280 nm (λ_{em} =320–500 nm) and λ_{ex} = 295 nm (λ_{em} = 320–540 nm). In PMEApp displacement experiment, 100 nM 2-(CI-ANT)-ANPpps were displaced from ACT by PMEApp at concentrations of 5 nM to 1 μ M. Direct fluorescence of MANTS was excited at 350 nm, and steady-state emission spectra were recorded from 380 to 550 nm. The final concentrations of ACT and CaM were 2.4 μ M each. Saturation experiments were performed using MANTS at concentration range from 10 nM to 500 nM; ACT and CaM were 300 nM each. Saturation curves were obtained by subtracting the fluorescence intensity at 430 nm after the addition of ACT from the maximal fluorescence (FRET) after the addition of ACT/CaM. Half-saturation concentration EC₅₀ was calculated using the Graphpad Prism 5 software (San Diego, CA, USA). Basal fluorescence in the presence of buffer alone was subtracted.

Assays with mACs—HEK cells stably expressing AC1, AC2, or AC5 were cultured and frozen as previously described.^[41,42] Cells were thawed and plated in white bottom 384-well plates (PerkinElmer, Shelton, CT). Inhibitor compounds (at concentration of 30 μ M) were added to cells and incubated at room temperature for 30 min. Then, the specific mAC stimulator (3 μ M A23187 for AC1, 100 nM PMA for AC2, and 300 nM forskolin for AC5) in 500 μ M 3-isobutyl-1-methylxanthine was added to the cells. Cells were incubated at room temperature for 1 h and cAMP accumulation was measured using Cisbio's dynamic 2 kit (Cisbio Bioassays, Bedford, MA) according to the manufacturer's instructions.

Supplementary Material

Refer to Web version on PubMed Central for supplementary material.

Acknowledgments

This work was supported by the IOCB research project RVO 61388963, by the Ministry of Interior of the Czech Republic (VG20102015046), Ministry of Education of the Czech Republic (NPU LO1302), Gilead Sciences (Foster City, CA, USA), NIH (MH101673), and Purdue University (West Lafayette, IN, USA).

References

1. Diavatopoulos DA, Cummings CA, Schouls LM, Brinig MM, Relman DA, Mooi FR. Plos Pathog. 2005; 1:e45. [PubMed: 16389302]
2. Pertussis vaccines: WHO position paper: Weekly Epidemiological Record. 2010; 85:385–400. [PubMed: 20939150]
3. Kilgore PE, Salim AM, Zervos MJ, Schitt HJ. Clin. Microbiol. Rev. 2016; 29:449–486. [PubMed: 27029594]
4. a) Tiwari, T.; Murphy, TV.; Moran, J. [accessed October 2015] Morbidity and Mortality Weekly Report. 2005 Dec 9. <http://www.cdc.gov/mmwr/preview/mmwrhtml/rr5414a1.htm> Wood N, McIntyre P. Pediatr. Resp. Rev. 2008; 9:201–212.

5. Bartkus JM, Juni BA, Ehresmann K, Miller CA, Sanden GN, Cassidy PK, Saubolle M, Lee B, Long J, Harrison AR Jr, Besser JM. *J. Clin. Microbiol.* 2003; 41:1167–1172. [PubMed: 12624047]
6. Wendelboe AM, Rie AV, Salmaso S, Englund JA. *Pediatr. Infect. Dis. J.* 2005; 24:S58–S61. [PubMed: 15876927]
7. a) Ladant D, Ullmann A. *Trends Microbiol.* 1999; 7:172–176. [PubMed: 10217833] b) Confer DL, Eaton JW. *Science.* 1982; 217:948–950. [PubMed: 6287574]
8. Glaser P, Sakamoto H, Bellalou J, Ullmann A, Danchin A. *EMBO J.* 1988; 7:3997–4004. [PubMed: 2905265]
9. a) Mock M, Ullmann A. *Trends Microbiol.* 1993; 1:187–192. [PubMed: 8143137] b) Ahuja N, Kumar P, Bhatnagar R. *Crit. Rev. Microbiol.* 2004; 30:187–196. [PubMed: 15490970] c) Shen Y, Zhukovskaya NL, Zimmer MI, Soelaiman S, Bergson P, Wang CR, Gibbs CS, Tang WJ. *Proc. Natl. Acad. Sci. USA.* 2004; 101:3242–3247. [PubMed: 14978283]
10. a) Martín C, Gómez-Bilbao G, Ostolaza H. *J. Biol. Chem.* 2010; 285:357–364. [PubMed: 19875442] b) Fisher R, Masin J, Bumba L, Pospisilova E, Fayolle C, Basler M, Sadilkova L, Adkins I, Kamanova J, Cerny J, Konopasek I, Osicka R, Laclerc C, Sebo P. *PLoS Pathog.* 2012; 8(4):e1002580. [PubMed: 22496638]
11. De Clercq A, Holý A, Rosenberg I, Sakuma T, Balzarini J, Maudgal PC. *Nature.* 1986; 323:464–467. [PubMed: 3762696]
12. a) De Clercq E, Holý A. *Nat. Rev. Drug Discovery.* 2005; 4:928–940. [PubMed: 16264436] b) De Clercq E. *Med. Res. Rev.* 2013; 33:1278–1303. [PubMed: 23568857]
13. a) Reiser H, Wang J, Chong L, Watkins WJ, Ray AS, Shibata R, Birkus G, Cihlar T, Wu S, Li B, Liu X, Henne IN, Wolfgang GHI, Desai M, Rhodes GR, Fridland A, Lee WA, Plunkett W, Vail D, Thamm DH, Jeraj R, Tumas DB. *Clin. Cancer Res.* 2008; 14:2824–2832. [PubMed: 18451250] b) Zídek Z, Potm šil P, Holý A. *Toxicol. Appl. Pharmacol.* 2003; 192:246–253. [PubMed: 14575642]
14. a) Keough DT, Hocková D, Rejman D, Špa ek P, Vrbková S, Kre merová M, Eng WS, Jans H, West NP, Naesens LM, de Jersey J, Guddat LW. *J. Med. Chem.* 2013; 56:6967–6984. [PubMed: 23927482] b) Eng WS, Hocková D, Špa ek P, Janeba Z, West NP, Woods K, Naesens LMJ, Keough DT, Guddat LW. *J. Med. Chem.* 2015; 58:4822–4838. [PubMed: 25915781]
15. a) Keough DT, Hocková D, Holý A, Naesens LM, Skinner-Adams TS, de Jersey J, Guddat LW. *J. Med. Chem.* 2009; 52:4391–4399. [PubMed: 19527031] b) Hocková D, Keough DT, Janeba Z, Wang TH, de Jersey J, Guddat LW. *J. Med. Chem.* 2012; 55:6209–6223. [PubMed: 22725979] c) Keough DT, Špa ek P, Hocková D, Tichý T, Vrbková S, Slav tínská L, Janeba Z, Naesens L, Edstein MD, Chavchich M, Wang TH, de Jersey J, Guddat LW. *J. Med. Chem.* 2013; 56:2513–2526. [PubMed: 23448281] d) Keough DT, Hocková D, Janeba Z, Wang T, Naesens L, Edstein MD, Chavchich M, Guddat LW. *J. Med. Chem.* 2015; 58:827–846. [PubMed: 25494538] e) Kaiser MM, Hocková D, Wang T-H, Draěínský M, Pořtová-Slavitínská L, Procházková E, Edstein MD, Chavchich M, Keough DT, Guddat LW, Janeba Z. *ChemMedChem.* 2015; 10:1707–1723. [PubMed: 26368337]
16. a) Zídek Z, Franková D, Holý A. *Antimicrob. Agents Chemother.* 2001; 45:3381–3386. [PubMed: 11709312] b) Zídek Z, Franková D, Holý A. *Int. J. Immunopharmacol.* 2000; 22:1121–1129. [PubMed: 11137619] c) Potm šil P, Kre merová M, Kmoní ková E, Holý A, Zídek Z. *Eur. J. Pharmacol.* 2006; 540:191–199. [PubMed: 16733050]
17. Guo Q, Shen Y, Lee Y-S, Gibbs CS, Mrksich M, Tang W. *EMBO J.* 2005; 24:3190–3201. [PubMed: 16138079]
18. Shen YQ, Zhukovskaya NL, Zimmer MI, Soelaiman S, Bergson P, Wang CR, Gibbs CS, Tang WJ. *Proc. Natl. Acad. Sci. USA.* 2004; 101:3242–3247. [PubMed: 14978283]
19. Shoshani I, Laux WHG, Périgaud Ch, Gosselin G, Johnson RA. *J. Biol. Chem.* 1999; 274:34742–34744. [PubMed: 10574942]
20. esnek M, Jansa P, Šmídková M, Mertlíková-Kaiserová H, Dra ínský M, Brust TF, Pávek P, Trejtnar F, Watts VJ, Janeba Z. *ChemMedChem.* 2015; 10:1351–1364. [PubMed: 26136378]
21. a) Šmídková M, Dvo áková A, Tlouš ová E, esnek M, Janeba Z, Mertlíková-Kaiserová H. *Antimicrob. Agents Chemother.* 2014; 58:664–671. [PubMed: 24145524] b) Pradere U, Garnier-Amblard EC, Coats SJ, Amblard F, Schinazi RF. *Chem. Rev.* 2014; 114:9154–9218. [PubMed: 25144792]

22. a) Gille A, Seifert R. *J. Biol. Chem.* 2003; 278:12672–12679. [PubMed: 12566433] b) Gille A, Lushington GH, Mou TC, Doughty MB, Johnson RA, Seifert R. *J. Biol. Chem.* 2004; 279:19955–19969. [PubMed: 14981084] c) Seifert R, Dove S. *Trends Microbiol.* 2012; 20:343–351. [PubMed: 22578665]
23. Hiratsuka T. *J. Biol. Chem.* 1985; 260:4784–4790. [PubMed: 3988736]
24. Göttle M, Dove S, Steindel P, Shen Y, Tang W, Geduhn J, König B, Seifert R. *Mol. Pharmacol.* 2007; 72:526–535. [PubMed: 17553924]
25. Holý A. *Collect. Czech. Chem. Commun.* 1978; 43:2054–2031.
26. a) Kuhn K, Owen DJ, Bader B, Wittinghofer A, Kuhlmann J, Waldmann H. *J. Am. Chem. Soc.* 2001; 123:1023–1035. [PubMed: 11456655] b) Hradilová L, Poláková M, Dvořáková B, Hajdúch M, Petruš L. *Carboh. Res.* 2012; 361:1–6.
27. Chen JJ, Cai X, Szostak JW. *J. Am. Chem. Soc.* 2009; 131:2119–2121. [PubMed: 19166350]
28. a) Allison BD, Phuong VK, McAtee LC, et al. *J. Med. Chem.* 2006; 49:6371–6390. [PubMed: 17034143] b) Twin H, Batey RA. *Org. Lett.* 2011; 6:4913–4916. c) Liu J, Deng X, Fitzgerald AE, Sales ZS, Vankatesan H, Mani S. *Org. Biomol. Chem.* 2011; 9:2654–2660. [PubMed: 21365101]
29. a) Kremerová M, Masojídková M, Holý A. *Collect. Czech. Chem. Commun.* 2004; 69:1889–1913. b) Kremerová M, Drašinský M, Hocková D, Holý A, Keough DT, Guddat LW. *Bioorg. Med. Chem.* 2012; 20:1222–1230. [PubMed: 22249123]
30. Vrbovská S, Holý A, Pohl R, Masojídková M. *Collect. Czech. Chem. Commun.* 2006; 71:543–566.
31. Jansa P, Baszczynski O, Drašinský M, Votruba I, Zídek Z, Bahador G, Stepan G, Cihlar T, Mackman R, Holý A, Janeba Z. *Eur. J. Med. Chem.* 2011; 46:3748–3754. [PubMed: 21664011]
32. a) Holý A, Rosenberg I. *Collect. Czech. Chem. Commun.* 1987; 52:2801–2809. b) Moffatt JG, Khorana HG. *J. Am. Chem. Soc.* 1961; 83:649–658.
33. Xu B, Stephens A, Kirschenheuter G, Greslin AF, Cheng X, Sennelo J, Cattaneo M, Zighetti ML, Chen A, Kim S, Kim HS, Bischofberger N, Cook G, Jacobson KA. *J. Med. Chem.* 2002; 45:5694–5709. [PubMed: 12477353]
34. Kim HS, Barak D, Harden TK, Boyer JL, Jacobson KA. *J. Med. Chem.* 2001; 44:3092–3108. [PubMed: 11543678]
35. Hackett M, Walker CB, Guo L, Gray MC, Van Cuyk S, Ullmann A, Shabonowith J, Hunt DF, Hewlett EL, Sebo P. *J. Biol. Chem.* 1995; 270:20250–20253. [PubMed: 7657593]
36. Iwaki M, Kamachi K, Konda T. *Infect. Immun.* 2000; 68:3727–3730. [PubMed: 10816536]
37. Birkus G, Wang R, Liu X, Kutty N, MacArthur H, Cihlar T, Gibbs C, Swaminathan S, Lee W, McDermott M. *Antimicrob. Agents Chemother.* 2007; 51:543–550. [PubMed: 17145787]
38. Luedtke CC, Andonian S, Igdoura S, Hermo L. *J. Histochem. Cytochem.* 2000; 48:1131–1146. [PubMed: 10898806]
39. Molecular Operating Environment (MOE). 2014:0901. Chemical Computing Group Inc. 1010 Sherbooke St. West, Suite #910. Montreal, QC, Canada, H3A 2R7: 2016.
40. Šolínová V, Kaiser MM, Lukáš M, Janeba Z, Kašík V. *J. Sep. Sci.* 2014; 37:295–303. [PubMed: 24259415]
41. Conley JM, Brand CS, Bogard AS, Pratt EPS, Xu RQ, Hockerman GH, Ostrom RS, Dessauer CW, Watts VJ. *J. Pharm. and Exp. Ther.* 2013; 347:276–287.
42. Conley JM, Brust TF, Xu R, Burris KD, Watts VJ. *J. Vis. Exp.* 2014; 83:e51218.

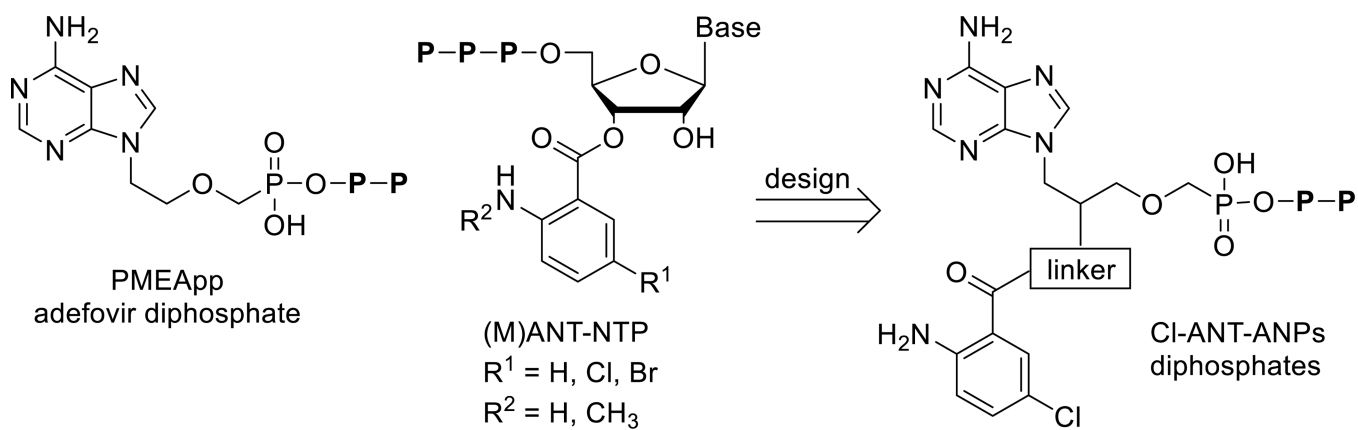


Figure 1.
Structures of adefovir diphosphate (PMEApp), (M)ANT-nucleotides and target CI-ANT-ANPpp analogues.

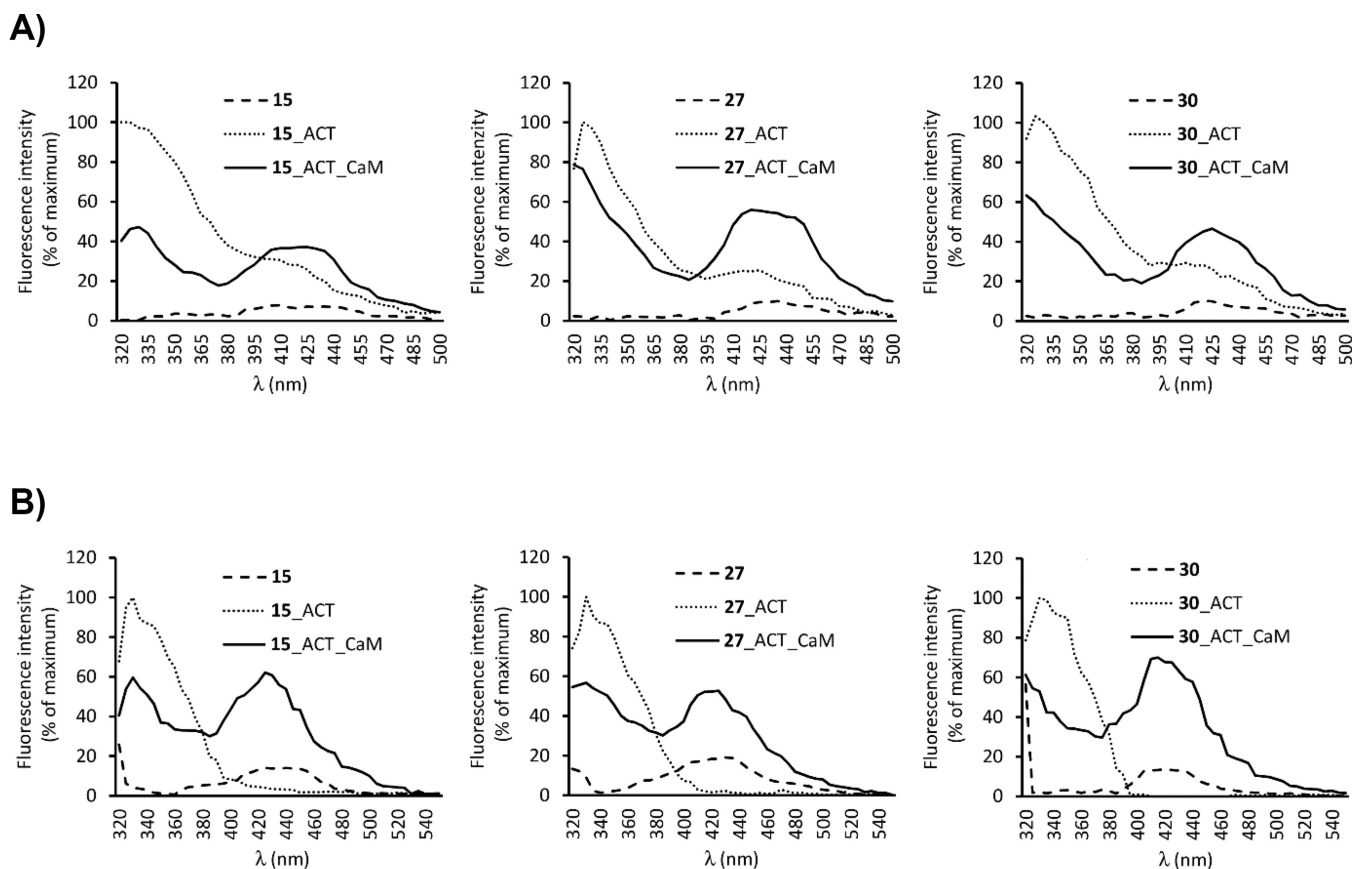


Figure 2.

Emission spectra representing binding of **15**, **27** and **30** to the catalytic site of ACT and the effect of calmodulin (CaM) on this process. Tested compounds were added to the assay buffer at final concentrations of 100 nM (**27**, **30**) or 300 nM (**15**) and the emission was scanned following the excitation at 280 nm (A) and 295 nm (B) – dashed lines. ACT (dotted lines) or ACT and CaM (solid lines) were added successively to yield final concentration of 300 nM. Data are expressed as a *percent of maximal fluorescence*. Superimposed recordings of representative experiments are shown.

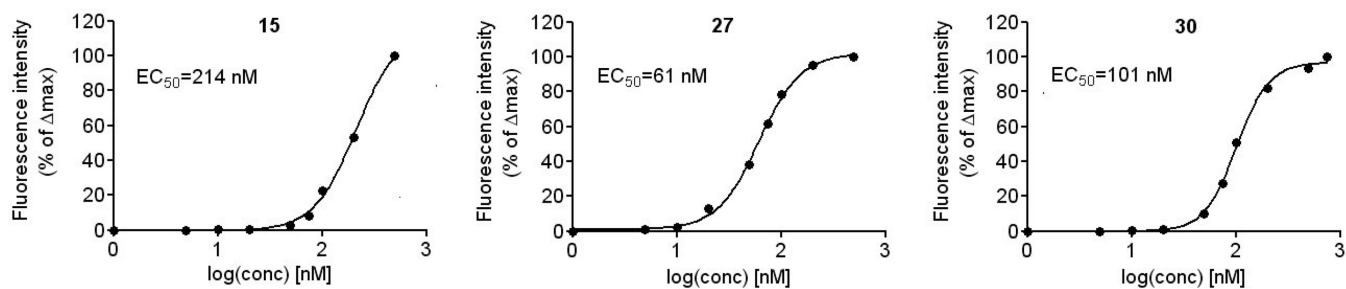


Figure 3.

Saturation of ACT active site with **15**, **27** and **30**. Final concentrations of ACT and CaM were 300 nM of each, nucleotides were used at final concentrations from 10 nM to 500 nM. The fluorescence increase at 430 nm was calculated by subtracting the fluorescence at 430 nm after the addition of ACT to Cl-ANT-ANPpp analogues from the maximal fluorescence at 430 nm following the final addition of CaM to the mixture. Similar data were obtained in three independent experiments. Half-saturation concentration EC₅₀ was calculated using GraphPad Prism 5.0 software.

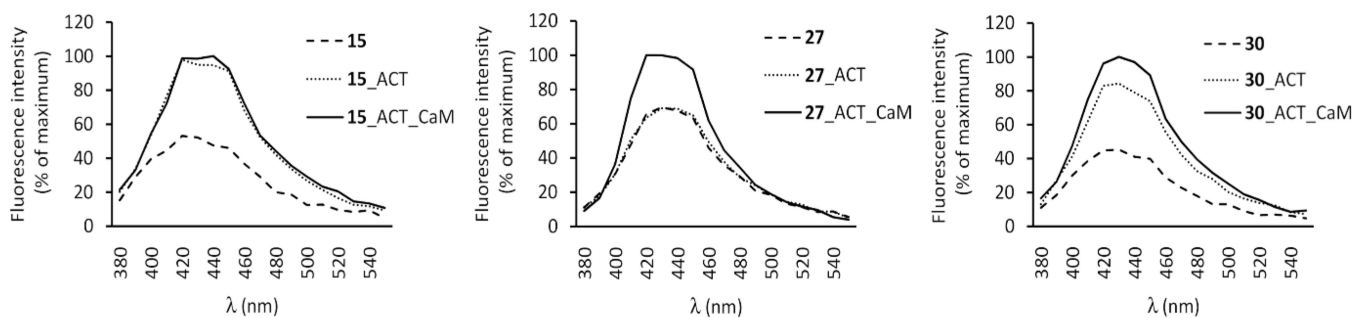


Figure 4.

Direct fluorescence of **15**, **27** and **30**. 100 nM of compound, 2.4 μ M ACT, and 2.4 μ M CaM were added to well in sequence. The excitation wavelength was 350 nm, and emission was immediately scanned from 380 to 550 nm. Superimposed recordings of a representative experiment are shown. Similar data were obtained in three independent experiments.

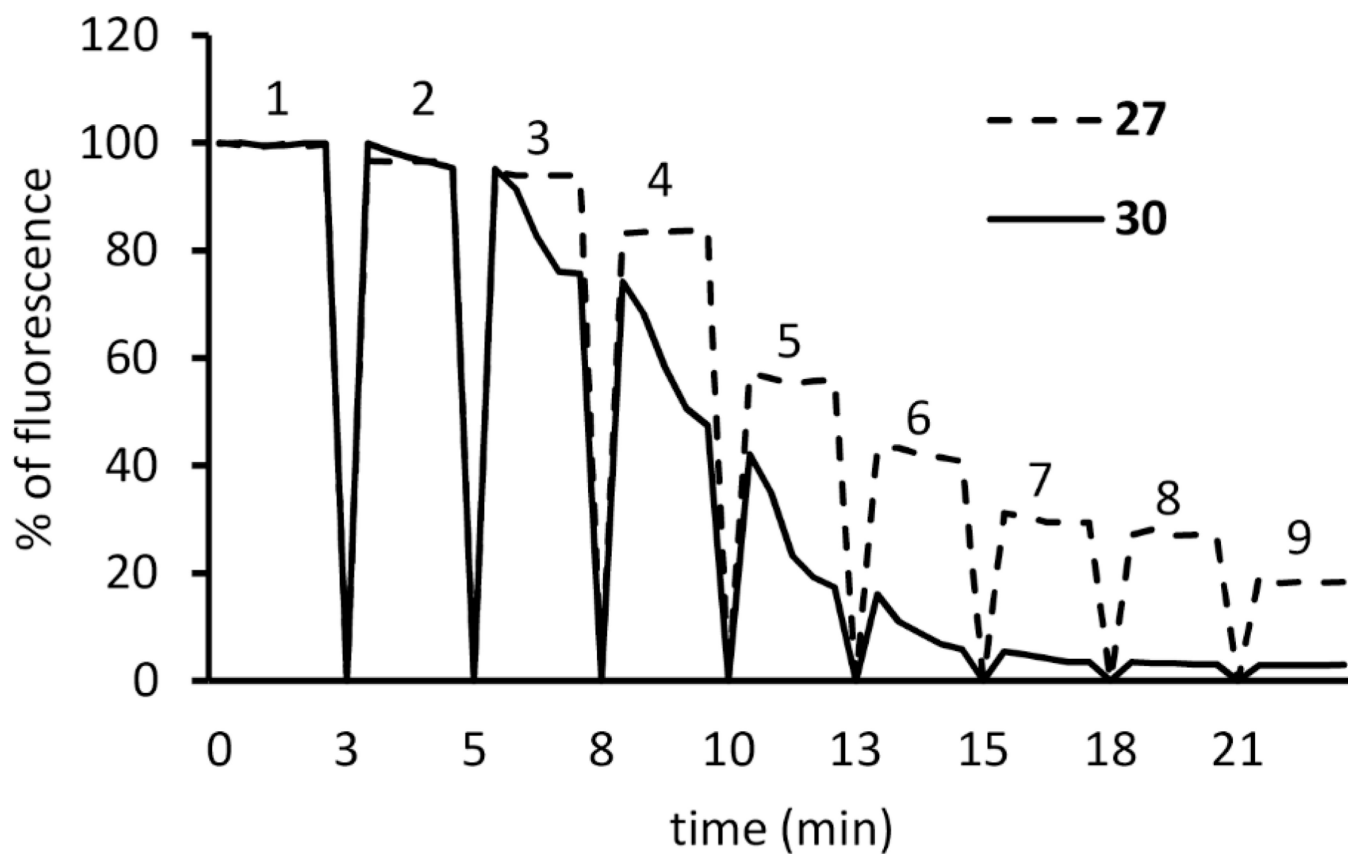


Figure 5.

Time-resolved activation of ACT by CaM and stepwise abolishment of FRET by PMEApp. Excitation wavelength was 280 nm and emission was detected at 430 nm over time. 100 nM of **27** or **30**, 300 nM ACT, 300 nM CaM, and PMEApp in the final concentrations of 0 nM (peak 1), 5 nM (peak 2), 25 nM (peak 3), 50 nM (peak 4), 100 nM (peak 5), 200 nM (peak 6), 300 nM (peak 7), 500 nM (peak 8) and 1000 nM (peak 9), were added in sequence. A record of a representative experiment is shown. Similar data were obtained in three independent experiments.

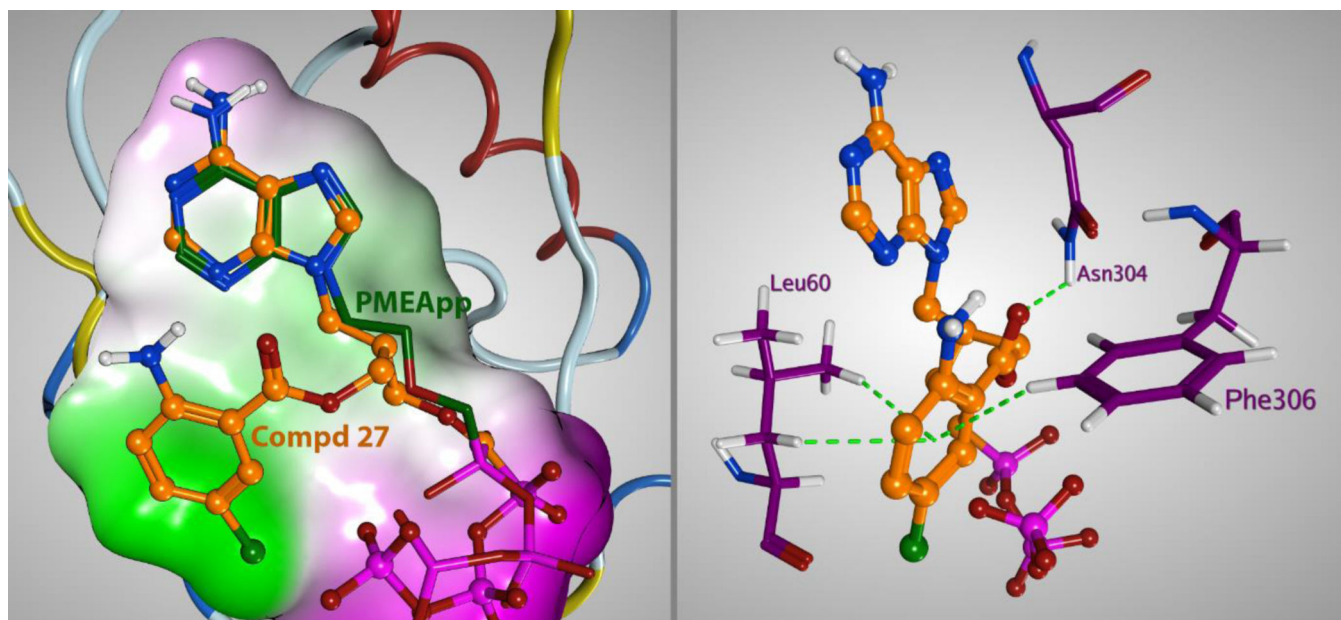
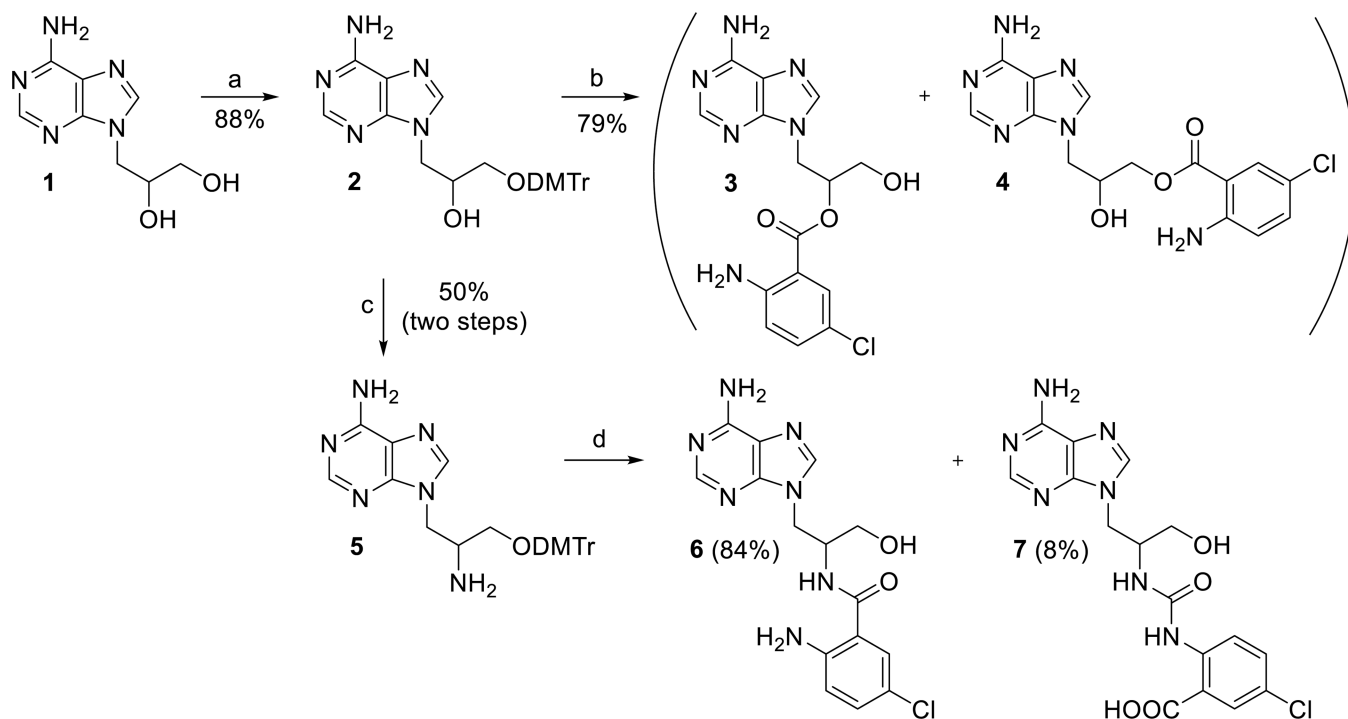
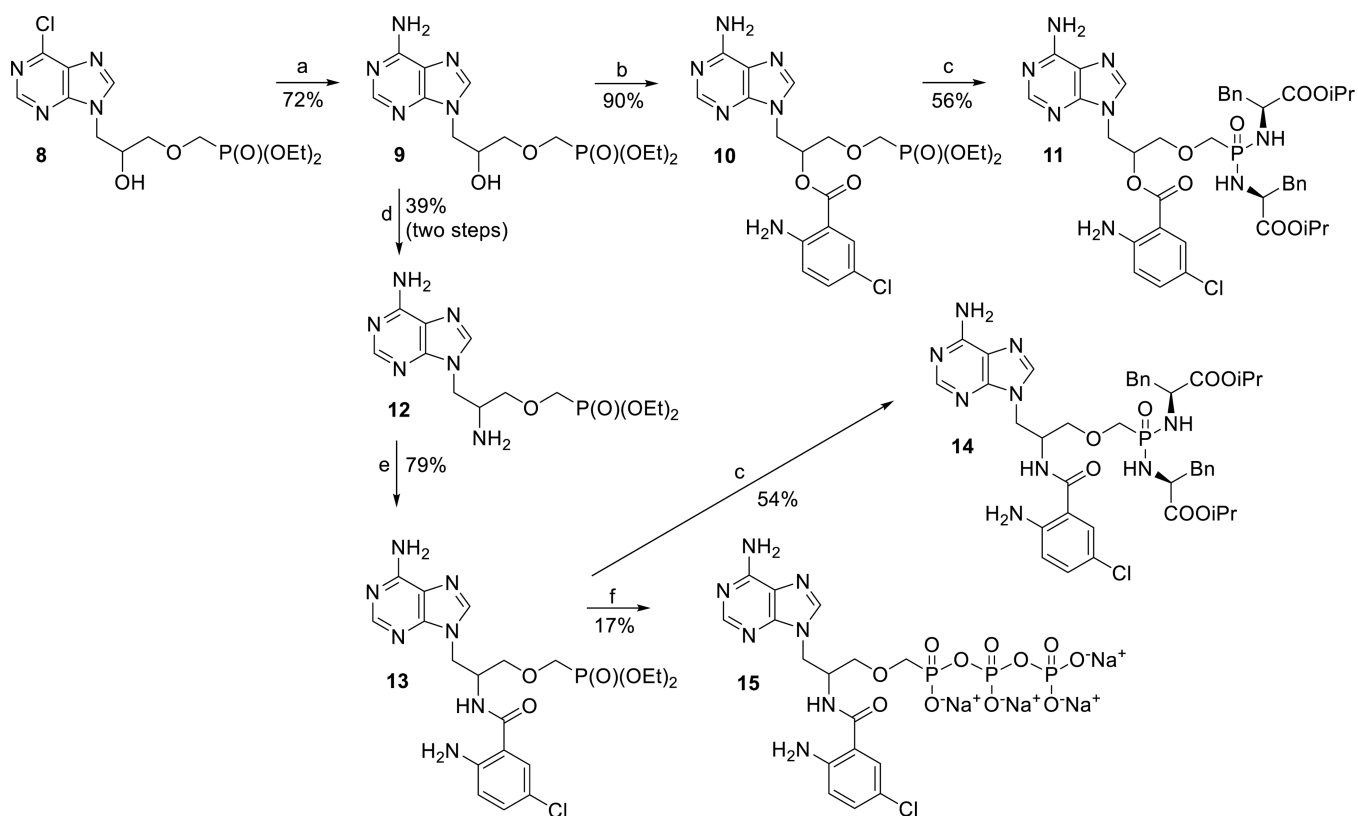


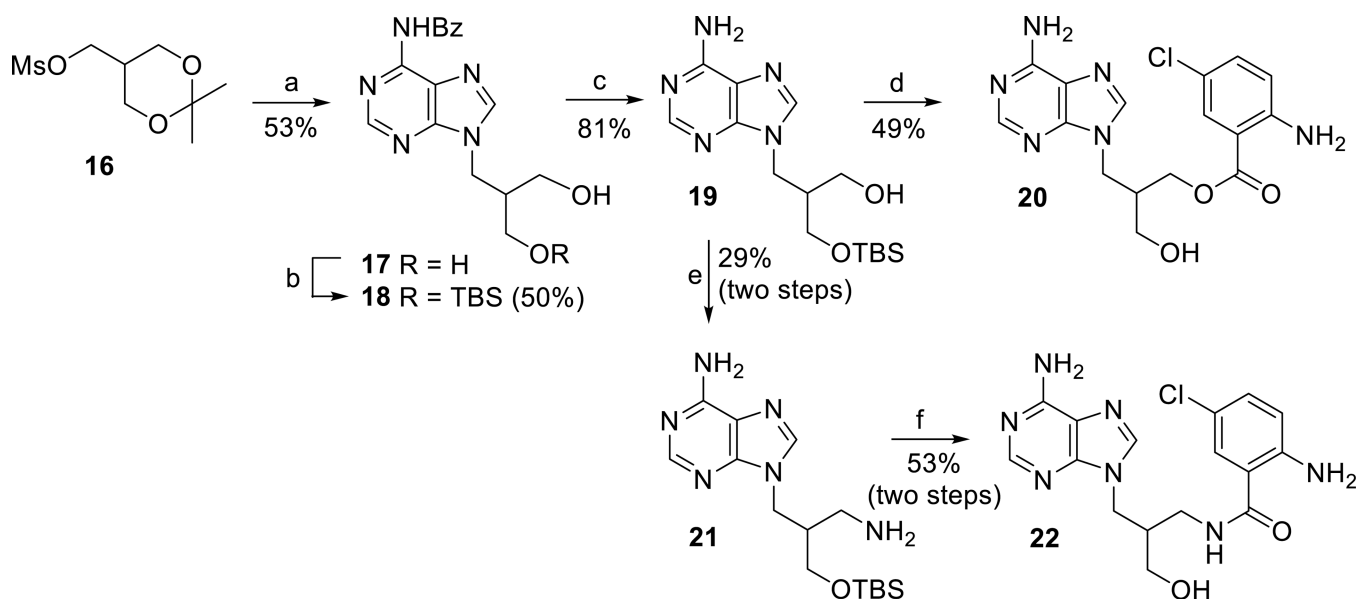
Figure 6. Left: Comparison of docking pose of compound **27** with PMEApp in the crystal structure (PDB 1ZOT).^[17] Right: Detail of binding of compound **27** in the ACT lipophilic pocket.

**Scheme 1.**

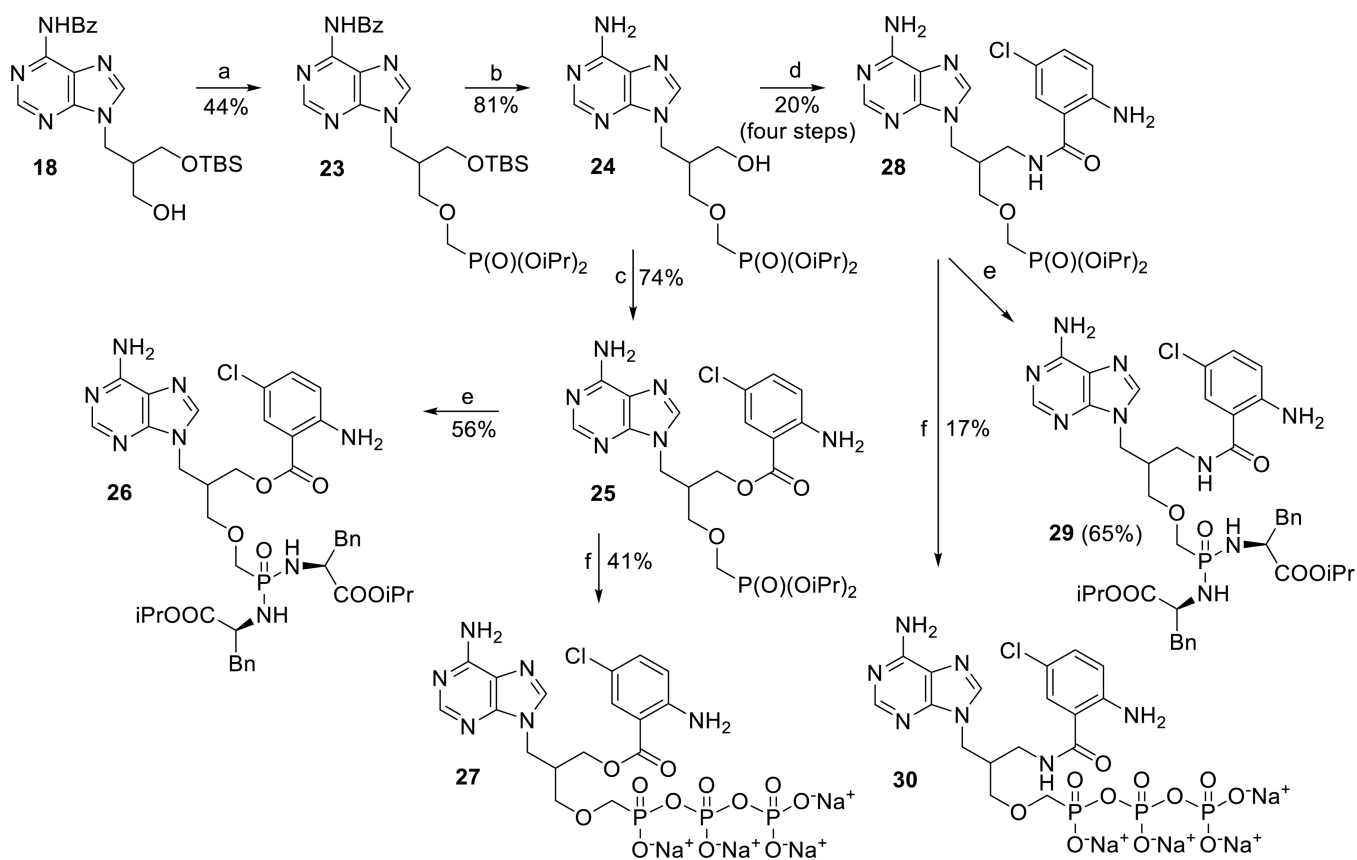
Synthesis of the Cl-ANT acyclic nucleosides. Reagents and conditions: a) DMTrCl, Py, RT, overnight; b) i) NaH, DMF, 5-chloroisatoic anhydride, 14 h; ii) 80% AcOH, RT, 2h; c) i) MsCl, Py, RT, 2 h; ii) NaN₃, DMF, HMPA, 100 °C, 14 h; iii) H₂/Pd/C, MeOH, RT, 24 h; d) i) 5-chloroisatoic anhydride, DMF, THF; ii) 80% AcOH, RT, 2h.

**Scheme 2.**

Synthesis of Cl-ANT-ANPs. Reagents and conditions: a) NH_3/EtOH , MW, 100°C , 30 min; b) 5-chloroisatoic anhydride, NaH, THF, RT, 24 h; c) TMSBr, Py, RT, 12 h, then L-phenylalanine isopropyl ester hydrochloride, TEA, 2,2'-dipyridyldisulfide, PPh_3 , Py, 70°C , 72 h; d) i) MsCl, Py, RT, 2 h; ii) NaN_3 , DMF, HMPA, RT, 5 days; iii) $\text{H}_2/\text{Pd/C}$, MeOH, RT, 12 h; e) 5-chloroisatoic anhydride, DMF, THF, DMAP, RT, overnight; f) i) TMSBr, Py, RT, 14 h; ii) morpholine, t-BuOH, DCC, H_2O ; III) tributylammonium pyrophosphate, DMSO, RT, 48 h.

**Scheme 3.**

Synthesis of Cl-ANT acyclic nucleosides with extended linker. Reagents and conditions: a) i) N^6 -benzoyladenine, NaH, DMF, 60 °C, 14 h; ii) 80% AcOH, 60 °C, 30 min; b) TBSCl, imidazole, DMF, RT, 14 h; c) 1M NaOMe/MeOH, MeOH, RT, 16 h; d) i) 5-chloroisatoic anhydride, NaH, DMF, 80 °C, 3 h; ii) 80% AcOH, 50 °C, 8 h; e) i) MsCl, Py, RT, 2 h; ii) NaN₃, DMF, RT, 5 days; iii) H₂/Pd/C, MeOH, RT, 14 h; f) i) 5-chloroisatoic anhydride, DMF, THF, DMAP, RT, 16 h; ii) 80% AcOH, 50 °C, 2 h.

**Scheme 4.**

Synthesis of Cl-ANT-ANPs derivatives with extended linker. Reagents and conditions: a) $\text{pTsOCH}_2\text{P}(\text{O})(\text{O}i\text{Pr})_2$, $\text{Mg}(\text{tBuO})_2$, DMF, 60°C , 72 h; b) TBAF, THF, RT, 16 h; c) 5-chloroisatoic anhydride, NaH, DMF, 50°C , 48 h; d) i) MsCl, Py, RT, 2 h; ii) NaN_3 , DMF, RT, 5 days; iii) $\text{H}_2/\text{Pd/C}$, MeOH, RT, 14 h; iv) 5-chloroisatoic anhydride, DMF, THF, DMAP, RT, 16 h; e) TMSBr, Py, RT, 12 h, then L-phenylalanine isopropyl ester hydrochloride, TEA, 2,2'-dipyridyldisulfide, PPh_3 , Py, 70°C , 72 h; f) i) TMSBr, Py, RT, 14 h; ii) morpholine, *t*-BuOH, DCC, H_2O ; III) tributylammonium pyrophosphate, DMSO, RT, 48 h.

Table 1IC₅₀ values of Cl-ANT-ANPpp for ACT and EF.

Compound	IC ₅₀ [nM] ^[a] ACT Sigma	IC ₅₀ [nM] ^[a] ACT Enzo	IC ₅₀ [nM] ^[a] EF
PMEApp	16.0 ± 0.2	13.6 ± 4.7	11.5 ± 2.6
15	294 ± 5	263 ± 37	68.9 ± 18.2
27	77.0 ± 18.1	198 ± 24	622 ± 124
30	90.5 ± 1.1	47.0 ± 0.7	140 ± 15

^[a]Data are the mean of at least three independent experiments.

Author Manuscript

Author Manuscript

Author Manuscript

Author Manuscript

Table 2

ACT inhibition and cytotoxic effects of bisamidate prodrugs of 5-chloroanthraniloyl-substituted acyclic nucleoside phosphonates in J774A.1 cells.

Compound	IC ₅₀ [μM] ^[a]	Viability [%] ^[b]
3 + 4	> 15	ND
6	> 15	ND
7	> 15	ND
11	> 15	ND
14	> 15	ND
20	> 15	ND
22	> 15	ND
26	12.1 ± 1.3	110
29	> 15	ND

^[a]Data are the mean ± SD of at least three independent experiments.

^[b]Data are the percent cell viability at a fixed prodrug concentration (10 μM) versus untreated control; ND: not determined.

Table 3

Mammalian AC1, AC2 and AC5 inhibition with with prepared Cl-ANT-compounds at concentration of 30 μ M). SQ22536 is a non-selective P-site inhibitor and SKF83566 is a selective inhibitors of AC2.^[41]

Compound	% of control ^a		
	AC1	AC2	AC5
3+4	180 \pm 21	147 \pm 15	97 \pm 8
6	163 \pm 34	161 \pm 16	98 \pm 14
7	178 \pm 31	164 \pm 23	110 \pm 16
11	168 \pm 12	159 \pm 30	103 \pm 10
14	118 \pm 12	172 \pm 34	121 \pm 23
20	122 \pm 15	146 \pm 10	114 \pm 18
22	156 \pm 23	149 \pm 26	101 \pm 5
26	94 \pm 10	149 \pm 27	97 \pm 11
29	189 \pm 15	193 \pm 48	118 \pm 18
SKF83566	95 \pm 9	-2 \pm 4	83 \pm 10
SQ22536	102 \pm 25	84 \pm 5	64 \pm 1

^aThe AC-inhibition data are expressed as % \pm S.E.M. of the control response (100%) in two independent experiments.